

Effects of TiO₂ Particles Size and Heat Treatment on Friction Coefficient and Corrosion Performance of Electroless Ni-P/TiO₂ Composite Coatings

Elina Esmaeel Nad and Maryam Ehteshamzadeh

*Department of Materials Science and Engineering, Faculty of Engineering,
P. O. Box 76175-133, Shahid Bahonar University of Kerman, Jomhoori Blvd., Kerman, Iran,
e-mail: ehtesham@uk.ac.ir*

The effects of the titanium dioxide (TiO₂) particles size on the friction coefficient and corrosion performance of the Ni-P/TiO₂ composite coatings before and after heat treatment at 400°C for 1h have been investigated. Pin-on-disc analysis results have revealed that the highest and the lowest friction coefficients belonged, respectively, to the simple Ni-P coating and the Ni-P/TiO₂ composite coating containing TiO₂ particles of the average size of 0.1 μm ($\mu \sim 0.62$ against 0.52). Eventually, a relative reduction in the corrosion resistance and the friction coefficient (as low as $\mu \sim 0.38$) have been observed after heat treatment of Ni-P and Ni-P/TiO₂ composite coatings.

Keywords: particle-reinforcement, friction, corrosion, EIS.

УДК 621.7

INTRODUCTION

Electroless deposition, a long-used process, an autocatalytic reduction of metals and alloys, is an attractive and alternative method of producing coatings with high Ni content; it has been known to form a thin and uniform deposit on the substrate when compared to electroplating [1].

The idea of codepositing various second phase particles in electroless nickel matrix and thereby taking advantages of their inherent uniformity, harden ability, wear and corrosion resistance, has led to the development of electroless nickel composite coatings. Many composite coatings are characterized by an amorphous or crystalline nickel matrix into which oxides such as NiO, Sc₂O₃, Fe₂O₃, RuO₂, Al₂O₃ and TiO₂ are incorporated [2, 3]. Other chemical compounds can also be codeposited with the nickel matrix, e.g. SiC, BN or PTFE [4, 5].

Incorporation of nano-sized particles within Ni-P autocatalytic coatings has greatly improved their properties thus imparting new functional features to the coating performance, which finally has widened their application in different fields. One of those particles, TiO₂, has attracted tremendous interest in the research community due to its wide application in engineering [6]. This material is widely used because of its high refractive index [7]. However, so far little attention has been paid to the incorporation of TiO₂ nanoparticles in the Ni matrix [8]. Composite coatings of the Ni matrix with a stable inorganic TiO₂ oxide offer the synergistic advantage of the metal matrix that is conductive and corrosion resistant and the oxide, which may enhance the corrosion and wear resistance or catalytic properties of the system [9]. In composite materials, the TiO₂ phase, with its high strength and high hardness, can

serve as an effective reinforcement to strengthen the composite and increase its hardness and wear resistance. The Ni-P plates containing TiO₂ composite have improved physical-chemical characteristics [10]. The right configuration of the size, morphology and structure of the TiO₂ nanoparticles should be specified for every particular application.

The given paper considers a very important effect of adding second-phase particles into simple electroless coatings and partially fills the gap in the insufficient number of investigations on the effect of the second-phase particle size and of heat treatment on wear and corrosion performance of composite coatings.

EXPERIMENTAL DETAILS

Preparation of substrate

Mild steel specimens (5 × 2 × 0.5 cm³) were used as substrates of electroless Ni-P coatings. The samples were polished by successive emery papers (grit numbers: 120, 500, 1000 and 2400). Having been cleaned by distilled water and ethanol for removing any pollution, the specimens were soaked in acetone for 30 minutes. The procedure was followed by immersing the specimens in the sulfuric acid solution for 30 seconds in order to activate the samples surfaces. All chemicals were of the analytical grade (Merck).

Plating bath and coating process

The compositions of electroless baths are given in Table 1. Magnetic stirrer was used to get uniform suspension of particles in the solution. In each case, 250 mL of suspension containing Ti particles and an optimized amount of the anionic surfactant sodium dodecyl sulfate (SDS) [11] were stirred for 12h on a

magnetic stirrer to improve wettability of the particles. The TiO_2 powder was added to the composite coating bath, separately, in three average sizes: 20 nm, 0.1 μm and 0.3 μm , which, respectively, led to the composite coatings with symbols D1, D2 and D3 thereafter. As to D, it showed a simple Ni-P coating.

Table 1. Simple and composite coating bath composition and operating conditions for electroless coating

Composition	Simple Ni-P bath	Ni-P/ TiO_2 bath
$\text{NiSO}_4 \cdot 6\text{H}_2\text{O}$ (g/L)	21	21
$\text{NaH}_2\text{PO}_2 \cdot \text{H}_2\text{O}$ (g/L)	25	25
Lactic acid (mL)	24	24
Propionic acid (mL)	3	3
TiO_2 (g/L)	–	2
Pb acetate (g/L)	0.004	0.004
Thio urea (g/L)	0.002	0.002
Surfactant (g/L)	–	0.2 (SDS)
Temperature	$89 \pm 2^\circ\text{C}$	$89 \pm 2^\circ\text{C}$
pH	4.6 ± 0.2	4.6 ± 0.2
Duration(min)	40	40

Heat treatment

To study the effect of heat treatment on the properties and structure of the composite coatings, the samples were subjected to the annealing heat treatment. This was carried out in an argon atmosphere furnace at 400°C for 1h. The samples were allowed to cool in the furnace after the heat treatment.

Equipment

Scanning electron microscope (SEM) CamScan MV2300 was employed to study surface morphologies. Also, the deposits compositions were analyzed by the energy dispersive X-ray (EDX) analyzer. The X-ray diffraction (XRD) analyzer equipment (Philips, Xpert, Cu K_α radiation) with X'pert Highscore 1.0d software was used for detecting the phases. Microhardness of the Ni-P based coatings was measured using a microhardness equipment (Struers Duramin, Denmark), with a diamond pyramid as an indenter and 50g load, 15s loading duration and five trials per each sample.

Electrochemical measurements were done using an EG&G Potentiostat/Galvanostat Model 263A accompanied with a frequency response analyzer Model 1025. A classical cell of three-electrodes was employed: a platinum electrode was a counter electrode, a saturated calomel electrode (SCE) was a reference electrode and the samples with an exposed area of 1 cm^2 were working electrodes. The potentiodynamic polarization curves were recorded in the range of -0.4 to 0.4 vs an open circuit potential with the scan rate of 1 mVs^{-1} . Electrochemical impedance spectroscopy (EIS) measurements were done in the

frequency range of 100 KHz-10 mHz and the perturbation amplitude was 5 mV. Aqueous solution of 3.5% NaCl was used as the corrosive media in electrochemical tests.

Friction and wear performance were studied using pin-on-disc equipment interfaced with a data acquisition system. For all tests, the sliding velocity was fixed at 0.024 m/s and the sliding distance was 100 m. The load applied was 10 N. No lubricant was used during the test. The pins were made of steel with hardness of 62 RC.

RESULTS AND DISCUSSION

Morphology and microstructure

Fig. 1(a-d) exhibits the SEM images of the composite coatings containing TiO_2 particles in different sizes. It can be seen that there are many spherical protrusions over the surface. It was observed that when increasing the size of TiO_2 particles, the coatings surfaces became softer and smoother. This can be interpreted by a higher agglomeration of small TiO_2 particles in D1 and D2 composite coatings, which led to a rougher surface.

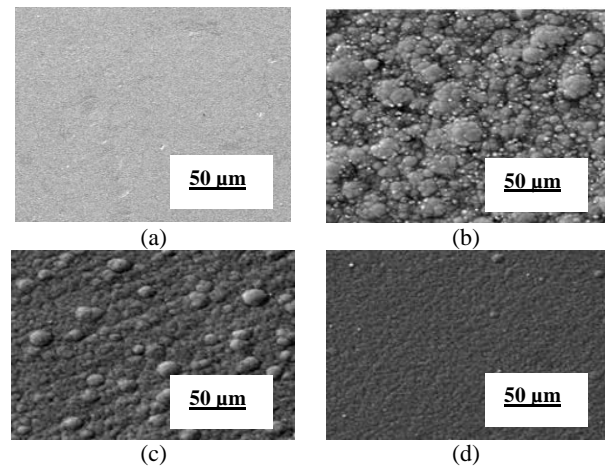


Fig. 1. SEM micrographs of electroless Ni-P and Ni-P/ TiO_2 composite coatings; (a) D, Ni-P coating; (b) D1, Ni-P/ TiO_2 in average size 20 nm; (c) D2, Ni-P/ TiO_2 of average size 0.1 μm ; (d) D3, Ni-P/ TiO_2 in average size 0.3 μm .

Fig. 2 shows a typical EDX spectrum of the composite coating D2. Similar results were observed for the composite coatings D1 and D3. Chemical compositions of the composite coatings are listed in Table 2. Incorporated TiO_2 particles in the Ni-P matrix for the composite coatings D1, D2 and D3 were found to be 2.9, 3.4 and 2.2 wt. %, respectively. It is obvious that the most incorporated amount of the TiO_2 particles was in the composite coating D2. In general, the incorporation of second phase particles in electroless Ni-P matrix depends on two factors: particles impingement on the electrode surface and the remaining time of the particles on the electrode surface [12]. Lower incorporation of the averaged sized – 20 nm and 0.3 μm , TiO_2 particles

in composite coatings D1 and D3, respectively, can be ascribed to either a relatively small or very large size of the particles, which are believed to be swept away from the surface, as compared to the particles in the averagely sized (0.1 μm) D2. Despite the presence of the surfactant SDS, another inevitable fact is agglomeration of nano-sized particles, which most probably occurs in the composite coating containing TiO_2 particles of the average size 20 nm, as is D1.

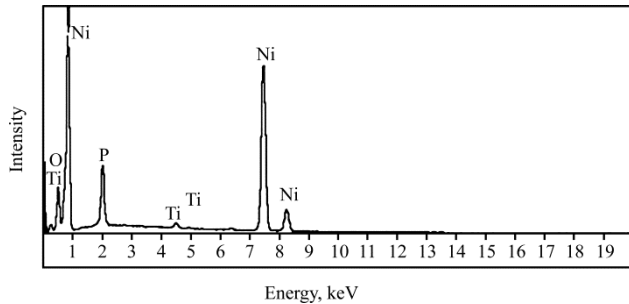


Fig. 2. Typical energy dispersive X-ray analysis of electroless Ni-P/ TiO_2 composite coating containing TiO_2 particles of average size 0.1 μm .

Table 2. Composition of electroless Ni-P and Ni-P/ TiO_2 composite coatings

Type of coating	TiO_2 particles average size	Ni (wt.%)	P (wt.%)	TiO_2 (wt.%)
D) Ni-P	–	89.1	10.9	–
D1) Ni-P/ TiO_2	20 nm	86.9	10.2	2.9
D2) Ni-P/ TiO_2	0.1 μm	87.0	9.6	3.4
D3) Ni-P/ TiO_2	0.3 μm	87.6	9.5	2.2

XRD patterns of the electroless Ni-P and Ni-P/ TiO_2 composite coatings, before and after heat treatment, are shown in Fig. 3. The amorphous nature of the electroless Ni-P matrix was evidenced in which crystalline TiO_2 particles are embedded. In the composite coatings, apart from a single broad peak corresponding to the amorphous Ni (111) plane at 45° , there are low intensity peaks of TiO_2 . After heat treatment, rapid transformation, from a disordered to an ordered arrangement, in the structure of the electroless Ni-P coatings of Ni_3P , Ni_5P_2 , Ni_7P_3 which resulted in several sharp peaks in the X-ray diffraction pattern.

Wear behavior

A tribological contact of solid bodies results in two major phenomena: friction and wear. Abrasion test results of simple and composite coatings are presented in Fig. 4. The Ni-P/ TiO_2 composite coatings showed improved wear resistance compare to a simple Ni-P deposit, with a friction coefficient (μ) ~ 0.62 . Among the composite coatings, D2 showed the lowest friction coefficient (~ 0.52)

which led to the best abrasion resistance. This could be explained by the amount of adsorbed TiO_2 particles in the deposit (3.4 wt.%), as evaluated by the EDX analysis. A higher percentage of the powder resulted in a reduced wear between the coating and the pin, thus enhancing the abrasion resistance of D2 in comparison with the other two composite coatings. The Friction Coefficients of D1 and D3 were estimated as ~ 0.55 and ~ 0.58 , respectively.

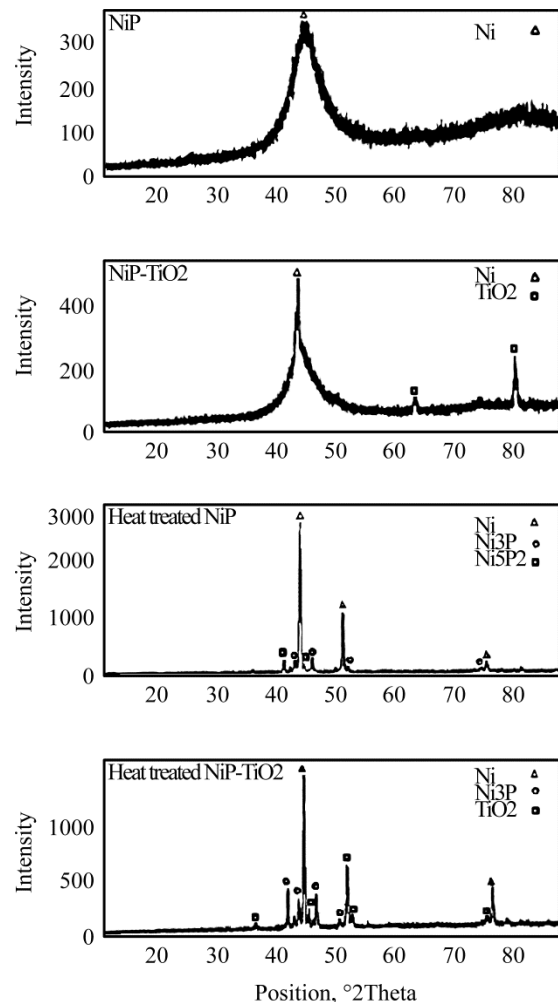


Fig. 3. XRD patterns of as-plated and heat treated Ni-P and typical Ni-P/ TiO_2 composite coating containing TiO_2 particles of average size 0.1 μm .

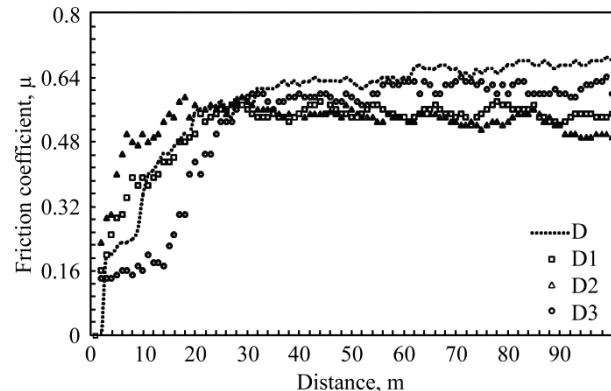


Fig. 4. Friction coefficient vs sliding distance of electroless Ni-P and Ni-P/ TiO_2 composite coatings; D) Ni-P coating, D1) Ni-P/ TiO_2 of average size 20 nm, D2) Ni-P/ TiO_2 of average size 0.1 μm , D3) Ni-P/ TiO_2 of average size 0.3 μm .

Fig. 5 displays Vickers microhardness values for as plated and heat treated electroless Ni-P and Ni-P/TiO₂ composite coatings. As is evident, increase in the size of TiO₂ particles led to a higher coating hardness. It can be recalled from the EDX analysis (Table 2) of the coatings that the amounts of phosphorus present in D, D1, D2 and D3 coatings, which is a crucial parameter in the electroless Ni-P plating, were 9.29, 10.2, 9.6 and 9.5 wt.%, respectively. It is clear that the larger the size of Ti particles, the smaller the amount of the deposited phosphorus. Because of the fact that phosphorus phase is a type of a soft phase, it affects the surface microhardness and can lead to smaller hardness values of the deposits. When electroless coatings are heated at a suitable temperature, formation and precipitation of the intermetallic Ni₃P, Ni₅P₂, Ni-P₃ phases occur, which act as barriers for dislocations movement, thereby hardness goes on increasing. This unique property of electroless alloys led to an extremely wide exploitations of such coatings for applications requiring wear and abrasion resistance.

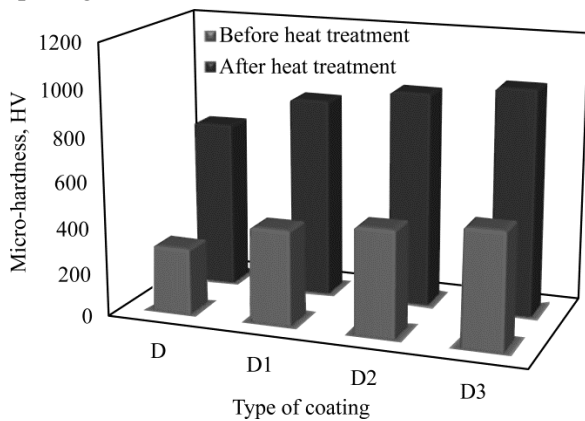


Fig. 5. Hardness profile of electroless Ni-P and Ni-P/TiO₂ composite coatings before and after heat treatment at 400°C for 1h; D) Ni-P coating, D1) Ni-P/TiO₂ of average size 20 nm, D2) Ni-P/TiO₂ of average size 0.1 μm, D3) Ni-P/TiO₂ of average size 0.3 μm.

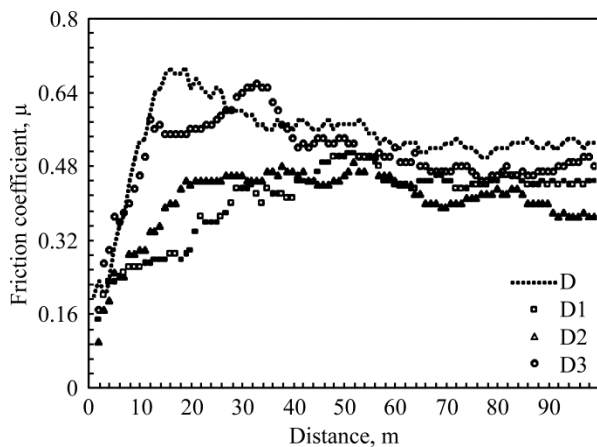


Fig. 6. Friction coefficient vs sliding distance of electroless Ni-P and Ni-P/TiO₂ composite coatings after heat treatment at 400°C for 1h; D) Ni-P coating, D1) Ni-P/TiO₂ of average size 20 nm, D2) Ni-P/TiO₂ of average size 0.1 μm, D3) Ni-P/TiO₂ of average size 0.3 μm.

As it is clear from Fig. 6, heat treatment affects the coatings abrasion behavior. A relative reduction of the friction coefficient values was observed after heat treatment. This can be accounted for by the creation of hard phases, such as Ni₃P, after heat treatment, which led to higher hardness values of coatings and therefore wear resistance. Besides, as was the case before heat treatment, the lowest friction coefficient is that of D2, which is as low as 0.38.

Corrosion performance

Fig. 7 shows polarization curves of electroless Ni-P and Ni-P/TiO₂ composite coatings containing TiO₂ particles of different sizes in the 3.5% sodium chloride solution; Table 3 lists their polarization parameters. It can be seen that the corrosion current density (i_{corr}) for a simple electroless Ni-P coating (D) is 2.04 μA/cm², whereas i_{corr} values for D1, D2 and D3 coatings are 2.54, 0.36 and 1.58 μA/cm², respectively. Among the four composite coatings, D2 showed the highest corrosion resistance. This can be attributed to the appropriate incorporation of Ti particles and their relevant distribution in the deposit, which are much better than at the other ones. This, in turn, can be attributed to the deposition of an enhanced barrier effect caused by the presence of TiO₂ particles in the Ni-P matrix and therefore a higher corrosion resistance of the deposit.

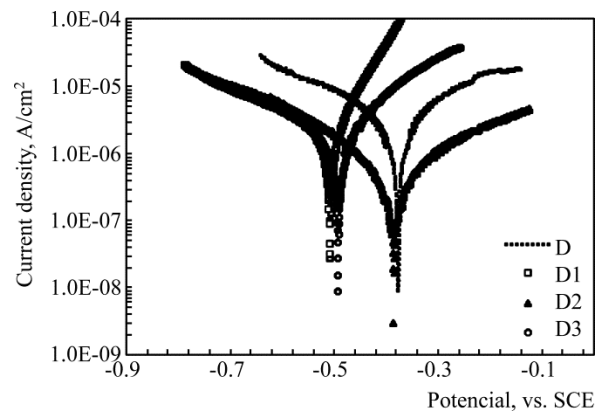


Fig. 7. Potentiodynamic polarization curves of electroless Ni-P and Ni-P/TiO₂ composite coatings in 3.5% NaCl aqueous solution; D) Ni-P coating, D1) Ni-P/TiO₂ of average size 20 nm, D2) Ni-P/TiO₂ of average size 0.1 μm, D3) Ni-P/TiO₂ of average size 0.3 μm.

Table 3. Polarization parameters of electroless Ni-P and Ni-P/TiO₂ composite coatings in 3.5% NaCl aqueous solution; D) Ni-P coating, D1) Ni-P/TiO₂ of average size 20 nm, D2) Ni-P/TiO₂ of average size 0.1 μm, D3) Ni-P/TiO₂ of average size 0.3 μm

Type of coating	i_{corr} (μA/cm ²)	E_{corr} (mV)	B_a (V/dec)	B_c (V/dec)	R_p (Ωcm ² ×10 ⁴)
D	2.046	-385	0.164	0.192	1.375
D1	2.543	-509	0.089	0.306	0.840
D2	0.361	-380	0.106	0.170	10.69
D3	1.580	-497	0.133	0.210	2.247

The lowest resistance was associated with D1 coating, which can be attributed to an effective exposure of the metallic area to the corrosive media. In D1 deposit, incorporation of extremely small TiO_2 particles can result in augmenting the particles agglomeration in the electroless bath and therefore in the composite film. This can be due to a big surface energy of ultrafine TiO_2 particles, which tends to pile them up severely, despite the presence of an appropriate surfactant SDS. Hence, the probability of localized corrosion in the D1 deposit is even higher than at a simple electroless plating.

On the other hand, more particle collisions in the electroless bath in the process of making D3 coating has led a lower content of TiO_2 in the deposit, thus causing a lower corrosion resistance of the deposit unlike the process in D2.

The impedance data of the coatings in the format of Nyquist and Bode plots are shown in Fig. 8. The results of the EIS studies also indicate a similar trend in the corrosion resistance like that observed in potentiodynamic polarization effects. The highest value of R_p for the D2 coating also implied that this type of a coating is more protective against corrosion, while the D1 deposit plot exhibited a low resistance in contrast with other films.

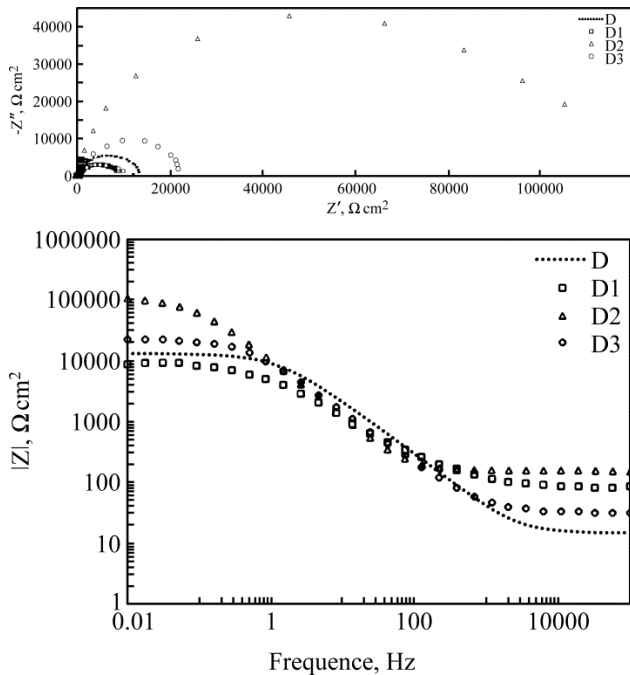


Fig. 8. EIS spectra of electroless Ni-P and Ni-p/ TiO_2 composite coatings in 3.5% NaCl aqueous solution; D) Ni-P coating, D1) Ni-P/ TiO_2 of average size 20 nm, D2) Ni-P/ TiO_2 of average size 0.1 μm , D3) Ni-P/ TiO_2 of average size 0.3 μm .

Corrosion behavior of the heat treated electroless coatings in the format of Nyquist and Bode plots are shown in Fig. 9. Extracted results of the EIS analysis are listed in Table 4. They are as follows: the highest R_p value refers to the D2 composite coating; in addition, the highest and the lowest corrosion resistance

demonstrated D2 ($i_{\text{corr}} = 1.419 \text{ A/cm}^2$) and D1 ($i_{\text{corr}} = 3.24 \text{ A/cm}^2$), respectively. The heat treated electroless Ni-P and Ni-p/ TiO_2 composite coatings exhibited larger i_{corr} values than the equivalent as-plated coatings. A higher corrosion resistance of as-plated coatings may be attributed to their amorphous nature. Amorphous alloys offer better resistance to corrosion attack than the equivalent polycrystalline materials because of the freedom from grain and grain boundaries [9].

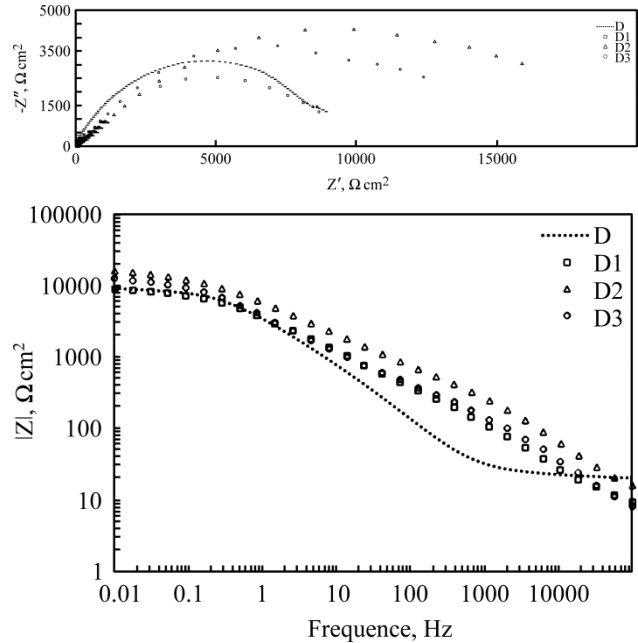


Fig. 9. EIS spectra of electroless Ni-P and Ni-p/ TiO_2 composite coatings in 3.5% NaCl aqueous solution after heat treatment at 400°C for 1h; D) Ni-P coating, D1) Ni-P/ TiO_2 of average size 20 nm, D2) Ni-P/ TiO_2 of average size 0.1 μm , D3) Ni-P/ TiO_2 of average size 0.3 μm .

Table 4. Polarization parameters of electroless Ni-P and Ni-p/ TiO_2 composite coatings in 3.5% NaCl aqueous solution after heat treatment at 400°C for 1h; D) Ni-P coating, D1) Ni-P/ TiO_2 of average size 20 nm, D2) Ni-P/ TiO_2 of average size 0.1 μm , D3) Ni-P/ TiO_2 of average size 0.3 μm

Type of coating	i_{corr} ($\mu\text{A/cm}^2$)	E_{corr} (mV)	R_p ($\Omega\text{cm}^2 \times 10^4$)
D	2.793	-495.0	0.889
D1	3.249	-485.8	0.867
D2	1.419	-546.2	1.586
D3	1.780	-551.3	1.235

After heat treatment, a mixture of crystalline nickel and nickel phosphide is created, therefore areas of different corrosion potentials are produced. This may leads to the formation of minute active/passive corrosion cells and consequently provoke an accelerated attack by an aggressive medium. The comparison of deposits demonstrates that the composite coating with the 20 nm particle size of TiO_2 has the lowest corrosion resistance, which is even less than with a simple Ni-P coating.

Fig. 10 schematically compares the corrosion behavior of the coatings before and after heat treatment.

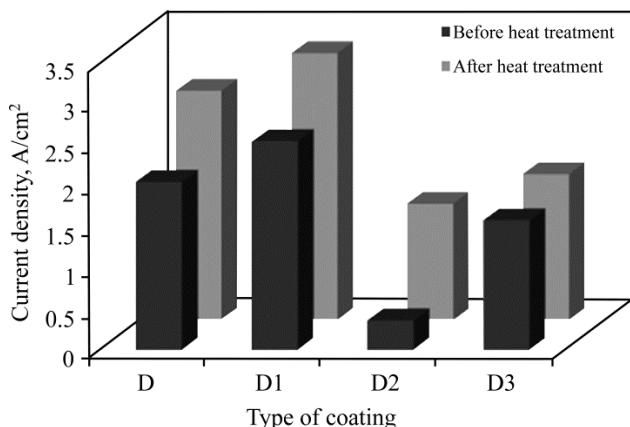


Fig. 10. Comparison in corrosion current densities of electroless Ni-P and Ni-P/TiO₂ composite coatings before and after heat treatment at 400°C for 1h; D) Ni-P coating, D1) Ni-P/TiO₂ of average size 20 nm, D2) Ni-P/TiO₂ of average size 0.1 μm, D3) Ni-P/TiO₂ if average size 0.3 μm.

CONCLUSIONS

1. Heavier agglomeration of TiO₂ particles was observed in the presence of 20 nm TiO₂ particles.

2. A larger and more uniform distribution of TiO₂ particles were found in the Ni-P/TiO₂ composite coatings containing TiO₂ particles of the average size of 0.1 μm.

3. The highest and the lowest friction coefficients were observed with the simple Ni-P and the Ni-P/TiO₂ composite coatings containing TiO₂ particles of the average size of 0.1 μm, respectively, ($\mu \sim 0.62$ against 0.52).

4. Heat treatment of the electroless Ni-P and Ni-P/TiO₂ at 400°C for 1h caused lowering of the friction coefficient, so that μ arrived ~ 0.38 in the electroless Ni-P/TiO₂ composite coatings containing TiO₂ particles of the average size of 0.1 μm.

5. A reduction in the corrosion resistance was observed in the coatings after heat treatment.

ACKNOWLEDGMENTS

The authors would like to thank Mr. Amir Farzaneh for his technical support.

REFERENCES

- Ranganatha S., Venkatesha T.V., Vathsala K. Development of Electroless Ni-Zn-P/nano TiO₂ Composite Coatings and their Properties. *Appl Surf Sci.* 2010, **256**(24), 7377–7383.
- Novakovic J., Vassiliou P., Samara K.L., Argyropoulos Th. Electroless Ni-P/TiO₂ Composite Coatings: Their Production and Properties. *Surf Coat Technol.* 2006, **201**, 895–901.

- Chen Wei, Gao Wei, He Yedong. Electrodeposition of So-enhanced Nanostructured Ni-TiO₂ Composite Coatings. *Surf Coat Technol.* 2010, **204**, 2493–2498.
- Ramalho A., Miranda J.C. Friction and Wear of Electroless NiP and Ni-P PTFE Coatings. *Wear.* 2005, **259**(7–12), 828–834.
- Allahkaram S.R., Honarvar Nazari M., Mamaghani S., Zarebidaki A. Characterization and Corrosion Behavior of Electroless Ni-P/nano-SiC Coating Inside the CO₂ Containing Media in the Presence of Acetic Acid. *Materials & Design.* 2011, **32**, 750–756.
- León O.A., Staia M.H., Hintermann H.E. Wear Mechanism of Ni-P-BN(h) Composite Autocatalytic Coatings. *Surf Coat Technol.* 2005, **200**, 1825–1829.
- Pokrant S., Irsen S. Crystal Structure of TiO₂ Nanoparticles. *Microsc Microanal.* 2008, **14**(2), 354–355.
- Abdel Aal A., Hassan Hanaa B., Abdel Rahim M.A. Nanostructured Ni-P-TiO₂ Composite Coatings for Electrocatalytic Oxidation for Small Organic Molecules. *J Electroanal Chem.* 2008, **619–620**, 17–25.
- Ramalho A., Miranda J.C. The Relationship between Wear and Dissipated Energy in Sliding Systems. *Wear.* 2006, **260**(4–5), 361–367.
- Novakovic J., Vassiliou P. Vacuum Thermal Treated Electroless NiP-TiO₂ Composite Coatings. *Electrochim Acta.* 2009, **54**(9), 2499–2503.
- Farzaneh A., Ehteshamzadeh M., Ghorbani M., Vazife Mehrabani J. Investigation and Optimization of SDS and Key Parameters Effect on the Nickel Electroless Coatings Properties by Taguchi Method. *J Coat Technol Res.* 2010, **7**, 547–555.
- Balaraju J.N., Kalavati K.S., Rajam. Influence of Particle Size on the Microstructure, Hardness and Corrosion Resistance of Electroless Ni-P-Al₂O₃ Composite Coatings. *Surf Coat Technol.* 2006, **200**(12–13), 3933–3941.

Received 20.12.12

Accepted 25.03.13

Реферат

В работе рассматривается влияние размера частиц двуокиси титана (TiO₂) на коэффициент трения и характеристики коррозии покрытий из сложного сплава Ni-P/TiO₂ до и после тепловой обработки при 400°C в течение 60 мин. Анализ на трение и износ по схеме «штифт-диск» показал, что наибольший и наименьший коэффициенты трения наблюдались при простом Ni-P покрытии и при сложном Ni-P/TiO₂, с частицами TiO₂ со средним размером 0,1 μm ($\mu \sim 0,62$ в отличие от 0,52). В действительности, относительное уменьшение сопротивления коррозии и коэффициента трения (до $\mu \sim 0,38$) наблюдалось после тепловой обработки покрытий как из Ni-P, так и из Ni-P/TiO₂.

Ключевые слова: укрупнение частиц, трение, коррозия, спектроскопия электрохимического импеданса.